

## Muon Decay: Measurement of the Transverse Polarization of the Decay Positrons and its Implications for the Fermi Coupling Constant and Time Reversal Invariance

N. Danneberg,<sup>1</sup> W. Fetscher,<sup>1,\*</sup> K.-U. Köhler,<sup>1</sup> J. Lang,<sup>1</sup> T. Schweizer,<sup>1</sup> A. von Allmen,<sup>1</sup> K. Bodek,<sup>2,†</sup> L. Jarczyk,<sup>2</sup> S. Kistryn,<sup>2</sup> J. Smyrski,<sup>2</sup> A. Strzałkowski,<sup>2</sup> J. Zejma,<sup>2</sup> K. Kirch,<sup>3,‡</sup> A. Kozela,<sup>4,†</sup> and E. Stephan<sup>5</sup>

<sup>1</sup>Institute for Particle Physics (IPP), ETH Zürich, 8093 Zürich, Switzerland

<sup>2</sup>Institute of Physics, Jagellonian University, Kraków, Poland

<sup>3</sup>Paul Scherrer Institut, CH-5232 Villigen-PSI, Switzerland

<sup>4</sup>H. Niewodniczanski Institute of Nuclear Physics, Kraków, Poland

<sup>5</sup>Institute of Physics, University of Silesia, Katowice, Poland

(Received 2 July 2004; revised manuscript received 28 October 2004; published 19 January 2005)

The two transverse polarization components  $P_{T_1}$  and  $P_{T_2}$  of the  $e^+$  from the decay of polarized  $\mu^+$  have been measured as a function of the  $e^+$  energy. Their energy averaged values are  $\langle P_{T_1} \rangle = (6.3 \pm 7.7 \pm 3.4) \times 10^{-3}$  and  $\langle P_{T_2} \rangle = (-3.7 \pm 7.7 \pm 3.4) \times 10^{-3}$ . From the energy dependence of  $P_{T_1}$  and  $P_{T_2}$  the decay parameters  $\eta$ ,  $\eta''$  and  $\alpha'/A$ ,  $\beta'/A$  are derived, respectively. Assuming only one additional coupling besides the dominant  $V-A$  interaction one gets improved limits on  $\eta$ ,  $\beta'/A$ , and the scalar coupling constant  $g_{RR}^S$ :  $\eta = (-2.1 \pm 7.0 \pm 1.0) \times 10^{-3}$ ,  $\beta'/A = (-1.3 \pm 3.5 \pm 0.6) \times 10^{-3}$ ,  $\text{Re}\{g_{RR}^S\} = (-4.2 \pm 14.0 \pm 2.0) \times 10^{-3}$ , and  $\text{Im}\{g_{RR}^S\} = (5.2 \pm 14.0 \pm 2.4) \times 10^{-3}$ .

DOI: 10.1103/PhysRevLett.94.021802

PACS numbers: 13.35.Bv, 11.30.Er, 12.60.-i, 13.88.+e

Muon decay,  $\mu^+ \rightarrow \bar{\nu}_\mu e^+ \nu_e$ , as a purely leptonic process, provides a precise source of information on the charged current weak interaction. It can be described by the most general, local four-fermion point interaction Hamiltonian [1]. It contains ten complex coupling constants to be determined by experiment. The observables can be expressed in terms of a chiral Hamiltonian in charge-changing form characterized by fields of definite handedness [2]. The matrix element is given by [3,4]

$$\mathcal{M} = \frac{4G_F}{\sqrt{2}} \sum_{\gamma, \varepsilon, \mu} g_{\varepsilon\mu}^\gamma \langle \bar{e}_\varepsilon | \Gamma^\gamma | (\nu_e)_n \rangle \langle \bar{\nu}_m | \Gamma_\gamma | (\mu)_\mu \rangle. \quad (1)$$

The index  $\gamma = S, V, T$  labels the type of interaction (four-scalar, four-vector, four-tensor), while the indices  $\varepsilon, \mu = R, L$  indicate the chirality ( $R$  for right-handed,  $L$  for left-handed) of the particle spinors. The standard model predicts  $g_{LL}^V = 1$ , with all other couplings being zero. In fact, with a selected set of  $\mu$  decay experiments it has been possible to *derive* a lower limit for  $g_{LL}^V$  and upper limits for the absolute values of all other nine coupling constants [3].

In a continuing effort to search for interactions beyond the standard model, we have measured the transverse polarization of the  $e^+$  from the decay of polarized  $\mu^+$ . Although the  $e^+$  are polarized mainly longitudinally ( $P_L = 0.998 \pm 0.045$ ) [5], the experimental limit  $\Delta P_L$  still allows for sizeable transverse polarization components  $P_{T_1}$  and  $P_{T_2}$ .  $\mathbf{P}_{T_1} \equiv P_{T_1} \cdot \hat{\mathbf{x}}_1$  lies in the plane defined by the  $\mu$  polarization  $\mathbf{P}_\mu$  and the  $e^+$  momentum  $\mathbf{k}_e$ ,  $\mathbf{P}_{T_2} \equiv P_{T_2} \cdot \hat{\mathbf{x}}_2$  is perpendicular to this plane. Their unit vectors  $\hat{\mathbf{x}}_1$  and  $\hat{\mathbf{x}}_2$ , respectively, are given by

$$\hat{\mathbf{x}}_2 = \frac{\mathbf{k}_e \times \mathbf{P}_\mu}{|\mathbf{k}_e \times \mathbf{P}_\mu|}, \quad \hat{\mathbf{x}}_1 = \hat{\mathbf{x}}_2 \times \frac{\mathbf{k}_e}{|\mathbf{k}_e|}. \quad (2)$$

Both  $P_{T_1}$  and  $P_{T_2}$  are functions of the  $e^+$  energy  $E$  and

depend on the decay parameters  $\eta$ ,  $\eta''$  and  $\alpha'/A$ ,  $\beta'/A$ , respectively [4,6–8]. A precise value of  $\eta$  is needed for a model-independent determination of  $G_F$ .  $P_{T_2}$ ,  $\alpha'/A$ , and  $\beta'/A$  all are zero if time reversal invariance holds. These parameters have been determined previously resulting in the energy averaged polarization components  $\langle P_{T_1} \rangle = (16 \pm 23) \times 10^{-3}$ ,  $\langle P_{T_2} \rangle = (7 \pm 23) \times 10^{-3}$ , and in  $\eta = (11 \pm 85) \times 10^{-3}$  [9].

Here we report first results of an improved experiment. Figure 1 shows a schematic view of the experimental setup to measure the transverse polarization from the angular distribution of annihilation photons. All the major parts of

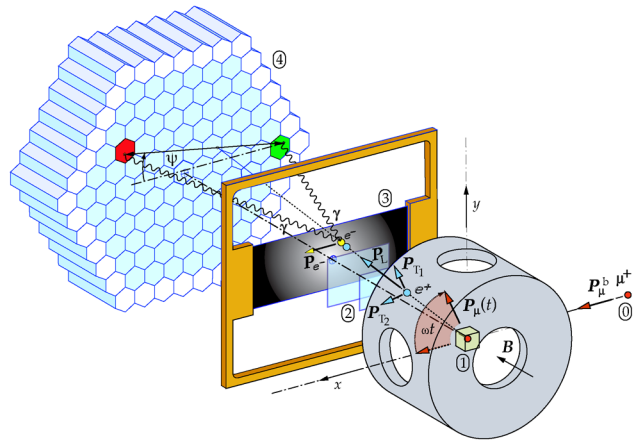


FIG. 1 (color online). Schematic view of the experimental setup. 0: Burst of polarized muons (angular frequency  $\omega$ , polarization  $P_\mu^b$ ). 1: Be stop target and precession field  $B$ . 2: Two plastic scintillation counters selecting decay positrons. 3: Magnetized Vacoflux 50<sup>TM</sup> foil serving as polarization analyzer. 4: Array of 127 BGO scintillators to detect the two  $\gamma$ 's from  $e^+$  annihilation-in-flight.

the previous experiment have been replaced by newly designed equipment in order to increase the event rate and reduce the systematic errors. This is described in detail elsewhere [10]. The experiment was performed at the  $\mu\text{E1}$  beamline at the Paul Scherrer Institute (PSI). A longitudinally polarized  $\mu^+$  beam ( $P_\mu^b \approx 91\%$ ) enters a beryllium stop target with bunches every 19.75 ns. The polarization  $\mathbf{P}_\mu(t)$  of the stopped muons precesses in a homogeneous magnetic field ( $B = 373.6 \pm 0.4$  mT) with the same angular frequency  $\omega$  as the accelerator radio frequency. This ensures that  $\mathbf{P}_\mu(t) \parallel \mathbf{P}_\mu^b$  for each newly arriving  $\mu^+$  bunch. Because of the burst width of 3.9 ns (FWHM) the polarization  $P_\mu(0)$  of the stopped  $\mu^+$  is reduced to  $(82 \pm 2)\%$ . A system of drift chambers (not shown) and two thin plastic scintillator counters  $T_0$  and  $T_1$  select decay  $e^+$  emitted into the direction of  $\mathbf{B}$ . A 1 mm thick magnetized Vacoflux 50<sup>TM</sup> foil (49% Fe, 49% Co, 2% V) in the central region with its polarized  $e^-$  ( $P_{e^-} = 7.2\%$ ) serves as polarization analyzer. The two  $\gamma$ 's from  $e^+$  annihilation in flight with the polarized  $e^-$  are selected by an array of 91 interior  $\text{Bi}_4\text{Ge}_3\text{O}_{12}$  (BGO) crystals with plastic veto counters in front of them to reject charged particles. The outer layer of 36 BGOs assists in an efficient collection of the deposited energy. Valid events are selected by using the correlation between the  $\gamma$  energies and their opening angle. The intensity distribution of the two  $\gamma$ 's has roughly the shape of the figure eight with a maximum in the direction of the bisector of  $\mathbf{P}_T(t)$  and the  $e^-$  polarization  $\mathbf{P}_{e^-}$  [11]. The precession of  $\mathbf{P}_\mu(t)$  implies a precession of  $\mathbf{P}_T(t)$ , while  $\mathbf{P}_{e^-}$  remains constant in time. Thus the intensity distribution of the  $\gamma$ 's also precesses with frequency  $\omega$ . For any given pair  $ij$  of BGO detectors we therefore ideally expect a signal for the normalized annihilation rate  $N_{ij}(t)$  in the form

$$N_{ij}(t) = 1 + a_{ij} \cos(\omega t + \delta_0) + b_{ij} \sin(\omega t + \delta_0), \quad (3)$$

where  $t$  denotes the time the  $e^+$  traverses counter  $T_0$  and  $\delta_0$  an instrumental phase common to all time spectra. The events are distributed in a time window of 39.5 ns total width, corresponding to two periods of the accelerator radio frequency. The Fourier coefficients  $a_{ij}$  and  $b_{ij}$  contain the complete information of the transverse positron polarization. In order to extract these coefficients the following two main obstacles have to be overcome:

(1) The  $e^+$  are emitted with energy  $E$  and transverse polarization vector  $\{P_{T_1}(E), P_{T_2}(E)\}$ . During their passage through the Be target, counters, and part of the magnetized foil they lose energy, change their direction, and their polarization precesses. Because of the finite depth of the Be target and due to the statistical nature of the energy loss,  $e^+$  of different original energy and polarization will end up with the same energy  $E'$  at the moment of annihilation. This is the energy as detected by measuring the two annihilation quanta. From the resulting transverse polar-

ization  $\{P_1(E'), P_2(E')\}$ , finally, the four decay parameters  $\eta$ ,  $\eta'$ ,  $\alpha'/A$ , and  $\beta'/A$  have to be deduced.

(2) The harmonic signal modulating the annihilation rate as given in Eq. (3) is accompanied by two other signals of the same frequency, but of different origin: One signal is due to the finite acceptance of the setup. The experiment selects  $e^+$  hitting a fiducial region of the analyzer foil ( $180 \times 160$  mm<sup>2</sup>) at a polar angle  $\chi < 14^\circ$  and an azimuthal angle  $\alpha$  with respect to the  $z$  and  $x$  axis, respectively. For  $\chi > 0^\circ$  there is a small [muon spin rotation ( $\mu\text{SR}$ )] decay asymmetry modulated by the precession  $\mathbf{P}_\mu(t)$ .

The other signal is a residual effect due to the differential nonlinearity of the time-to-digital converter (TDC) and the number of stopped  $\mu^+$  during one precession period, which is modulated by the finite width of the muon burst and the decay of a small fraction of the  $\mu^+$ . These two effects have been combined because they are independent of the rest of the experimental setup, particularly of  $P_{e^-}$  and the  $\mu\text{SR}$  decay asymmetry mentioned above.

The dependence of the three different contributions on the various observables plays an essential part in extracting the transverse polarization from the measured annihilation rate. The separation of the different contributions proceeds as follows: In order to minimize and control possible fluctuations of the Fourier coefficients the  $36.4 \times 10^6$  total valid annihilation events were subdivided into ten pairs of data sets of approximately equal size. Each pair  $\lambda$ , ( $\lambda = 1, \dots, 10$ ), consists of two consecutive measurements with opposite polarization  $P_{e^-}$ .

The Fourier coefficients ( $a_{\text{res}}^\lambda, b_{\text{res}}^\lambda$ ) of the residual effect were calculated by averaging the coefficients of pairs of measurements, which cancels effects of a possible transverse  $e^+$  polarization, as well as averaging over  $\alpha$ , which cancels the  $\mu\text{SR}$  asymmetry. The coefficients are found to be statistically consistent. Their mean value is  $a_{\text{res}} = (+7.44 \pm 0.24) \times 10^{-3}$ ,  $b_{\text{res}} = (-3.62 \pm 0.24) \times 10^{-3}$ .

The coefficients ( $a_{\mu\text{SR}}, b_{\mu\text{SR}}$ ) are proportional to  $\sin\chi$  and change sign for  $\alpha \rightarrow \alpha + 180^\circ$  (see Fig. 2). Therefore, it would be quite easy to eliminate this effect simply by accepting all events without regard to  $\alpha$ . It turns out, however, that actually it is essential for the experiment:

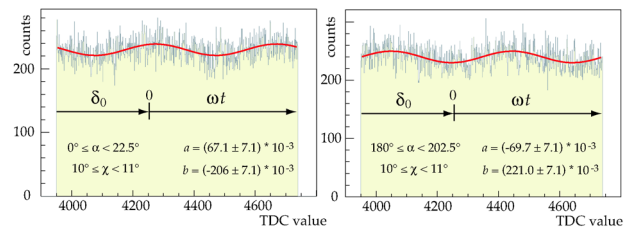


FIG. 2 (color online). Measured time spectra for two selected  $(\alpha, \chi)$  bins. The polar angular range is equal for both diagrams whereas the azimuthal angles differ by  $180^\circ$ . The solid lines and the coefficients  $a$  and  $b$  have been obtained from Fourier analysis. The origin of the  $\omega t$  axis is determined by the maximum of the rate for  $\alpha = 0$ .

The correlation between the maximum of the  $e^+$  flux at a given angle  $\alpha$  with the precessing  $\mathbf{P}_\mu(t)$  allows us to determine the phase angle  $\delta_0$  precisely. This establishes the calibration of the TDC channels with respect to  $\mathbf{P}_\mu$  which in turn allows to define the two polarization components  $P_1$  and  $P_2$  at the moment of annihilation. To achieve the best possible precision on  $\delta_0$ , events were sorted into 16 sectors  $\alpha_\nu$ , starting at  $0^\circ$ , and eight bins  $\chi_\kappa$ ,  $4^\circ \leq \chi_\kappa < 12^\circ$ . For each  $(\nu, \kappa)$  the Fourier coefficients were determined. After subtracting the residual coefficients ( $a_{\text{res}}, b_{\text{res}}$ ), dividing the result by  $\sin\chi_\kappa$ , and summing over  $\kappa$  one obtains the coefficients  $a_\nu, b_\nu$ . Figure 3 shows the results without (left) and with correction for the residual effect (right). Also shown is the statistical mean of all 16 coefficients (dots near center). With the properly determined coefficients (right) we obtain  $\langle a_{\mu\text{SR}} \rangle = (+0.9 \pm 2.0) \times 10^{-3}$ ,  $\langle b_{\mu\text{SR}} \rangle = (-1.2 \pm 2.0) \times 10^{-3}$  which demonstrates the high internal symmetry of the experiment. From these coefficients we obtain  $\delta_0 = 272.4^\circ \pm 0.5^\circ$ .

The transverse polarization, finally, is obtained for each pair  $\lambda$  from the difference of the Fourier coefficients with opposite  $P_e^-$ . This eliminates the residual contribution. Furthermore, we sum over all events from different detector pairs  $i, j$ , but identical azimuthal angle of orientation  $\psi$ , which averages over  $\alpha$ . This cancels the  $\mu\text{SR}$  decay asymmetry. The remaining coefficients contain only the signal of the transverse polarization [12]:

$$N_{\gamma\gamma}(t) = 1 + P_\mu P_e^- [P_1 G + P_2 H] \cos(\omega t + \delta_0) + P_\mu P_e^- [P_1 H - P_2 G] \sin(\omega t + \delta_0) \quad (4)$$

The analyzing powers  $G$  and  $H$  were derived from Ref. [13]. In contrast to  $P_1$  and  $P_2$  they depend not only on the sum  $u \equiv E_{\gamma_1} + E_{\gamma_2} = E'$  of the gamma energies, but also on  $v \equiv |E_{\gamma_1} - E_{\gamma_2}|$  as well as on  $\psi$ . Therefore the evaluation was subdivided even further, resulting in coef-

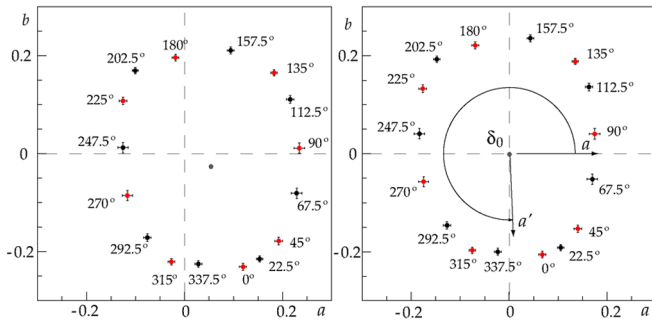


FIG. 3 (color online). Fourier coefficients ( $a_\nu, b_\nu$ ) obtained for each of the 16 sectors of the azimuthal angle  $\alpha$ . The left picture is without and the right picture is with the correction for the residual effect. The statistical mean of the coefficients of all 16 sectors is also shown as a dot near the center. After the correction it is well centered. The rotation of the axes ( $a, b$ ) by  $\delta_0$  to ( $a', b'$ ) eliminates the arbitrary phase and establishes the correlation of the signal with  $\mathbf{P}_\mu(t)$ .

ficients ( $a_{\nu\psi}^\lambda, b_{\nu\psi}^\lambda$ ). In each of these bins  $P_1(E')$  and  $P_2(E')$  were determined. For a given  $(\lambda, u)$  it was first verified that the values obtained for the various combinations of  $(\nu, \psi)$  were statistically consistent before combining them. The same procedure was applied with respect to the data sets  $\lambda$ . The resulting two polarization components  $P_1$  and  $P_2$  are shown as a function of  $E'$  in Fig. 4. All values are found to be consistent with 0.

The polarization components  $P_{T_1}$  and  $P_{T_2}$  at the moment of decay depend linearly on the decay parameters  $\eta, \eta''$ , and  $\alpha'/A, \beta'/A$ , respectively [4,6–8]. To derive these parameters from the measured distributions of  $P_1(E')$  and  $P_2(E')$  we have used a novel approach: With a modified GEANT3 [12,14] program we have generated four theoretical distributions [ $P_1(E'), P_2(E')$ ] in such a way that each was calculated by assigning a nonzero value to one of the four parameters and zero to the other three. Each individual  $e^+$  produced was fully polarized with respect to  $\mathbf{P}_{T_1}$  for  $\eta$  and  $\eta''$ , and to  $\mathbf{P}_{T_2}$  for  $\alpha'/A$  and  $\beta'/A$ , while the complete ensemble of  $e^+$  reproduced just the theoretical polarization as a function of  $E$ . The motion of these  $e^+$ , the deflection in the foil's magnetic field and the annihilation in the magnetized foil as well as the acceptance by the BGO detector array were then simulated, taking full account of the po-

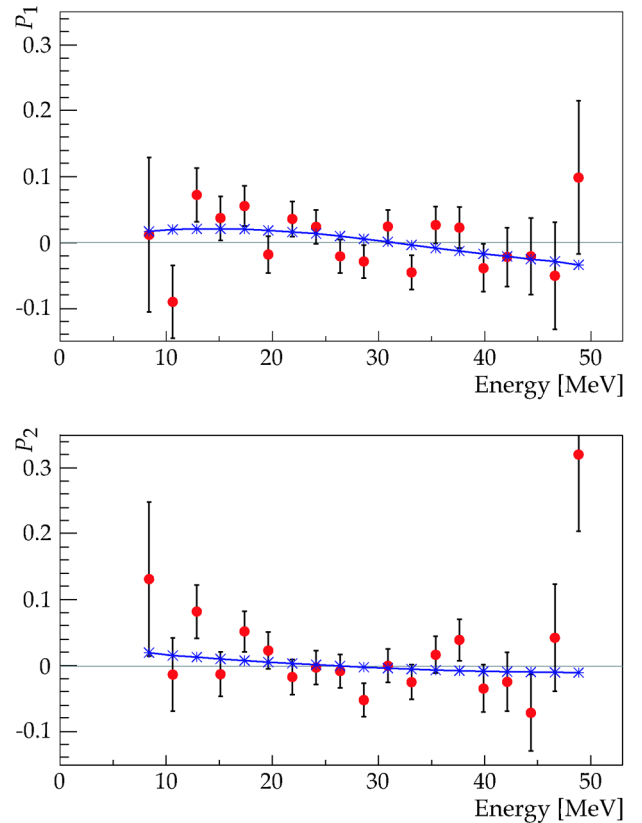


FIG. 4 (color online). Transverse positron polarization components  $P_1$  and  $P_2$  as a function of the  $e^+$  energy  $E'$  at the moment of annihilation. The curves are the fit to the data with the values obtained for  $\eta, \eta'', \alpha'/A$ , and  $\beta'/A$ .

TABLE I.  $V - A$  values and experimental results. All values, except  $\chi^2/\text{d.o.f.}$ , in units of  $10^{-3}$ . The correlation coefficients  $\rho_{ij}$  are all compatible with zero except the two coefficients listed. The errors are statistical and systematic.

|                           | $V - A$ | General analysis        | Restricted analysis     |
|---------------------------|---------|-------------------------|-------------------------|
| $\eta$                    | 0       | $71 \pm 37 \pm 5$       | $-2.1 \pm 7.0 \pm 1.0$  |
| $\eta''$                  | 0       | $105 \pm 52 \pm 6$      | $\equiv -\eta$          |
| $\alpha'/A$               | 0       | $-3.4 \pm 21.3 \pm 4.9$ | $\equiv 0$              |
| $\beta'/A$                | 0       | $-0.5 \pm 7.8 \pm 1.8$  | $-1.3 \pm 3.5 \pm 0.6$  |
| $\rho_{\eta\eta''}$       |         | 946                     | ...                     |
| $\rho_{\alpha'\beta'}$    |         | -893                    | ...                     |
| $\chi^2/\text{d.o.f.}$    |         | 46.2/33                 | 50.3/35                 |
| $\text{Re}\{g_{RR}^S\}$   | 0       | ...                     | $-4.2 \pm 14.0 \pm 2.0$ |
| $\text{Im}\{g_{RR}^S\}$   | 0       | ...                     | $5.2 \pm 14.0 \pm 2.4$  |
| $\langle P_{T_1} \rangle$ | -3      | $6.3 \pm 7.7 \pm 3.4$   |                         |
| $\langle P_{T_2} \rangle$ | 0       | $-3.7 \pm 7.7 \pm 3.4$  |                         |

larization dependence. The measured data were then fitted to a *linear* combination of the four simulated distributions. The extraction of the values and errors for  $\eta$ ,  $\eta''$ ,  $\alpha'/A$ , and  $\beta'/A$  is straightforward. The main systematic errors are due to uncertainties in the energy calibration, the energy loss and the background. Radiative corrections to the polarization are small [15,16] except at very low energies and have been neglected.

Table I shows the results of the general and of a restricted analysis. The average polarization components  $\langle P_{T_1} \rangle$  and  $\langle P_{T_2} \rangle$  have been calculated from the values of  $\eta$ ,  $\eta''$ , and  $\alpha'/A$ ,  $\beta'/A$ , respectively.

Based on the most general four-fermion contact interaction ("general analysis") the parameter  $\eta$  is given by [8]

$$\eta = \frac{1}{2} \text{Re}\{g_{LL}^V g_{RR}^{S*} + g_{RR}^V g_{LL}^{S*} + g_{LR}^V (g_{RL}^{S*} + 6g_{RL}^{T*}) + g_{RL}^V (g_{LR}^{S*} + 6g_{LR}^{T*})\}. \quad (5)$$

With  $g_{LL}^V \approx 1$ , and all other  $g_{e\mu}^V \approx 0$  [3], one can simplify Eq. (5) considerably by neglecting all terms quadratic in nonstandard couplings. This amounts to assuming one additional coupling beyond  $V - A$ . Then only two independent parameters remain ("restricted analysis"):

$$\eta = \text{Re}\{g_{RR}^S/2\}, \quad \beta'/A = -\text{Im}\{g_{RR}^S/4\}. \quad (6)$$

Here,  $g_{RR}^S$  is a scalar coupling with right-handed  $\mu$  and  $e$ .

The Fermi coupling constant  $G_F$  is generally derived assuming an exclusive  $V - A$  interaction, which amounts to setting  $\eta = 0$ . However,  $G_F$  depends on  $\eta$  [7,8]:

$$G_F \approx G_F^{V-A} \left(1 - 2\eta \frac{m_e}{m_\mu}\right), \quad (7)$$

where  $m_e/m_\mu$  is the mass ratio of electron and muon. Taking  $\eta$  into account increases the relative error  $\Delta G_F/G_F$  from  $9 \times 10^{-6}$  to  $360 \times 10^{-6}$  (general analysis) respective to  $68 \times 10^{-6}$  (restricted analysis). By extending the analysis beyond the general four-fermion local inter-

action  $P_{T_1}$  is found to depend also on a possible tensor interaction with coupling  $g_{RR}^T$  [17]. It leads to the same energy dependence of  $P_{T_1}$  as  $\eta$  and therefore cannot be distinguished from  $\eta$  by this measurement.

We note that our results on  $\alpha'/A$ ,  $\beta'/A$  (and deduced from these,  $\langle P_{T_2} \rangle$  and  $\text{Im}\{g_{RR}^S\}$ ) are the only experimental data sensitive to the violation of time reversal invariance for a purely leptonic *reaction*. In contrast to the violation of time reversal invariance in the neutral kaon system [18], a T-odd observable in muon decay would be due to an interference between two couplings with different phase angles and thus be an unambiguous signal of new physics beyond the standard model.

The results of our polarization measurements are in agreement with the standard model. The limits on  $\langle P_{T_1} \rangle$  and  $\langle P_{T_2} \rangle$  have been improved by a factor of 3, the limits on the four decay parameters  $\eta$ ,  $\eta''$ ,  $\alpha'/A$  and  $\beta'/A$  by a factor of 2. No evidence for the violation of time reversal invariance has been found.

We are grateful for the help of several PSI groups, especially D. George with the magnet group, the PSI workshop, the machine crew, and the "Hallendienst". This project was supported in part by the Swiss National Science Foundation and by the Polish Committee for Scientific research under Grant No. 2P03B05111.

\*Electronic address: fetscher@phys.ethz.ch

†Also at IPP, ETH Zürich, 8093 Zürich, Switzerland

- [1] L. Michel, Proc. Phys. Soc. London, Sect. A **63**, 514 (1950).
- [2] K. Mursula and F. Scheck, Nucl. Phys. **B253**, 189 (1985).
- [3] W. Fetscher, H.J. Gerber, and K.F. Johnson, Phys. Lett. B **173**, 102 (1986).
- [4] Particle Data Group, S. Eidelman *et al.*, Phys. Lett. B **592**, 410 (2004).
- [5] H. Burkard *et al.*, Phys. Lett. **150B**, 242 (1985).
- [6] T. Kinoshita and A. Sirlin, Phys. Rev. **108**, 844 (1957).
- [7] F. Scheck, Phys. Rep. **44**, 187 (1978).
- [8] W. Fetscher and H.J. Gerber, in *Precision Tests of the Standard Electroweak Model* edited by P. Langacker, (World Scientific, Singapore, 1995), p. 657.
- [9] H. Burkard *et al.*, Phys. Lett. **160B**, 343 (1985).
- [10] I.C. Barnett *et al.*, Nucl. Instrum. Methods Phys. Res., Sect. A **455**, 329 (2000).
- [11] F. Corriveau *et al.*, Phys. Lett. B **129**, 260 (1983).
- [12] W. Fetscher *et al.*, (to be published).
- [13] W. McMaster, Rev. Mod. Phys. **33**, 8 (1958).
- [14] CERN Computing and Networks Division - Application Software Group, CERN Program Library Long Writeup W5013, 1994.
- [15] M. Fischer, S. Groote, J.G. Komer, and M.C. Mauser, Phys. Rev. D **67**, 113008 (2003).
- [16] M. T. Mehr and F. Scheck, Nucl. Phys. **B149**, 123 (1979).
- [17] M. V. Chizhov, hep-ph/0405073.
- [18] CPLEAR, A. Angelopoulos *et al.*, Phys. Lett. B **444**, 43 (1998).